THE SNS FRONT END ACCELERATOR SYSTEMS*

John Staples, Daniel Cheng, Martin Fong, James Greer, Matthew Hoff,
Roderich Keller, Kurt Kennedy, Matthaeus Leitner, Robert MacGill,
Daryl Oshatz, Alessandro Ratti, Justin Remais, Steve Virostek
Lawrence Berkeley National Laboratory, Berkeley California, USA 94720

Abstract

The Spallation Neutron Source front end comprises a 35-70 mA volume H^- source, a multi-element electrostatic LEBT including chopping and steering, a 402.5 MHz RFQ with low output emittance and a 2.5 MeV MEBT also including chopping. The beam duty factor is 6%, with possible extension to 12%. This system, along with an LANL-supplied 1 GeV linac and a BNL-supplied storage ring, provides an average beam power of 1-2 MW to an ORNL and ANL-supplied neutron target and beam instruments facility. The current status of the front end design is described, along with results of several R&D projects leading to the final design.

1 INTRODUCTION

Over the last year the SNS design has undergone two DOE reviews and the project is expected to receive authorization for construction start. This paper reports on physics and engineering progress since the last report[1]. Hardware models have been built to test various subsystems, and some technical systems are now moving into prototype engineering design stages.

2 ION SOURCE

The design of the SNS prototype H^- ion source will be based on experiences gained with the SNS R&D ion source number 1, which is currently mounted on an ion source test stand at LBNL. A schematic of such an rf-driven (2 MHz) multicusp H^- ion source is shown in figure 1. A detailed design of this ion source has already been described elsewhere[2] .

Last year the ion source development was mainly concentrated on the extraction system[3]. Because of the high electron fraction in the beam extracted from a volume H^- ion source, an efficient electron removal scheme is essential for the 6% duty factor operation of the SNS H^- extraction system. We have chosen a novel design which deflects most electrons back to the ion source by a strong (1300 Gauss) magnetic field across the extraction hole as described in reference[4]. Only a small electron leakage current, which diffuses through the strong magnetic field, has to be dumped at a downstream electrode. To further reduce this unavoidable power load, we have added an intermediate electrode between the plasma outlet and the extractor electrode as shown in figure 2. All electrons leaking out of the magnetic deflector will be caught on this intermediate electrode, which has only a 3kV potential difference to the ion source potential.

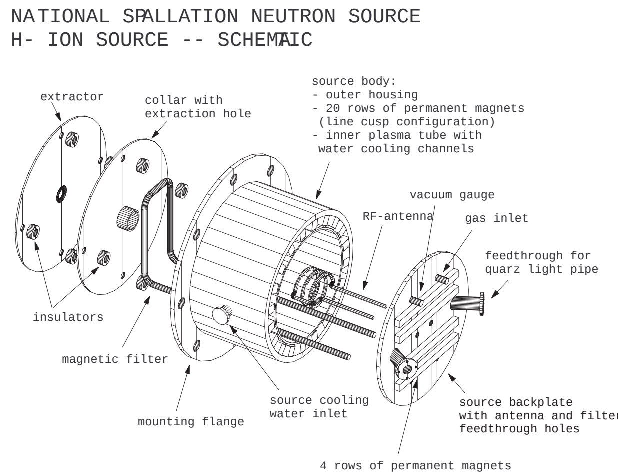

Figure 1: Ion Source Cross Section

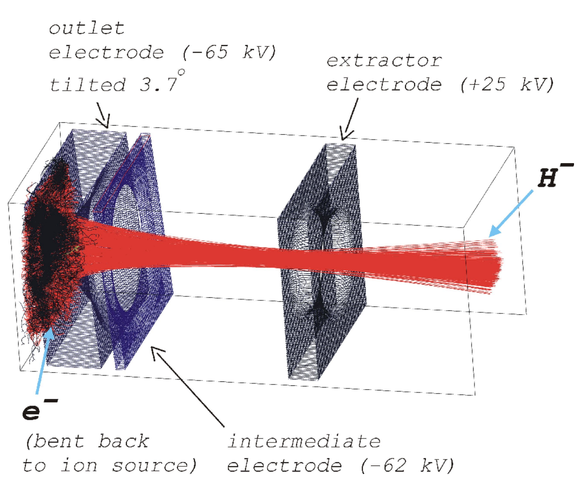

Figure 2: Ion Source Trajectories

The design of the magnetic field distribution across the extraction hole has been optimized with the 3D-ion-optics code KOBRA in combination with the 3D-magnet code TOSCA[5]. To compensate for the H^- ion beam deflection the outlet electrode must be tilted (see figure 2). It has been found that no transverse shift of the electrode is nec-

* This research is sponsored by the Lockheed Martin Energy Research Corporation under the U.S. Department of Energy, Contract No. DE-AC05-96OR22464, through the Lawrence Berkeley National Laboratory under Contract No. DE-AC03-76SF00098.

essary to inject a straight H^- ion beam into the LEBT. This feature eases the mechanical design and alignment of the SNS LEBT considerably.

3 LEBT

The Low Energy Beam Transport system has undergone some modification, described below. The all-electrostatic transport system provides a 65 keV beam to the RFQ entrance with a normalized emittance of less than 0.15π mm-mrad, with twiss parameters α = 1.6 and β = 6.5 cm.

Figure 3 shows a cross section of the LEBT electrode arrangement. The beam enters from the plasma generator off to the left, and is delivered to the RFQ through the tank endwall on the right.

The electrode geometry includes two pseudo-einzel lenses, allowing both α and β twiss parameters at the RFQ to be varied independently over a large range, and the last electrode, split into quadrants, allows beam angular steering by biasing the four segments, and beam chopping, by applying a $\pm$3 kV bipolar waveform to each segment, deflecting the beam in a stepped rotary pattern onto a four-segment beam stop. The length of the last focusing electrode has been extended to enhance the steering and chopping sensitivity. The electrically isolated four-segment beam stop, integrated into the RFQ endwall, will provide diagnostic signals of beam intensity and steering during the 35% of the time the beam is deflected away from the RFQ entrance by the LEBT chopper.

Tests on a prototype LEBT at LBNL show that the 3 kV bipolar chopper power supply rise/falltime is less than 40 nsec, and that the beam extinction time is 25-30 nsec.

The entire LEBT assembly is movable with respect to the RFQ for beam centering.

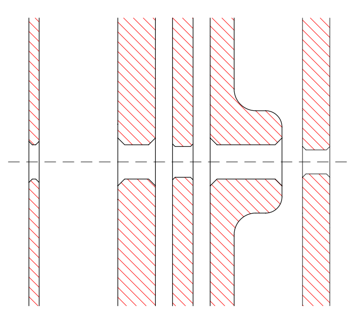

Figure 3: LEBT Cross Section

4 RFQ

The 3.7 meter-long RFQ accelerates 60 mA of H^- beam at greater than 95% transmission from 65 keV to 2.5 MeV. The r.f. duty factor is initially 6%, but the RFQ is capable of operating at 12% for a possible future upgrade of the facility to extend the average beam power to 4 MW. The RFQ comprises a single 402.5 MHz cavity, with pi-mode stabilizing loops[6] maintaining the quadrupole field symmetry in the presence of assembly errors. The one technical recommendation from the first DOE review committee was to increase the maximum current the RFQ could accommodate. This was done by increasing the peak field at the vanetips from 1.75 to 1.85 kilpatrick.

A r.f. cold model has been constructed and operated. It is full size in cross section and one-quarter length of the actual RFQ, with six pairs of pi-mode stabilizers, spaced 15.5 cm apart, as shown in figure 4. Perturbing one of the four quadrant frequencies by 1.53 MHz with plunger-type tuners causes a change in the quadrupole field balance by 2.7% worst case, with field levels in the remaining quadrants varying less. This substantial field stability will provide good field balance with normal mechanical assembly errors.

The pi-mode stabilizers move the quadrupole operating frequency down by 11 MHz and the two degenerate dipole modes up by 36 MHz from the non-stabilized cavity frequencies, with a resulting quadrupole-dipole separation of 35 MHz. No longitudinal stabilization is provided. The RFQ is five free-space wavelengths long, comparable to the JHF RFQ[6], which has no longitudinal stabilization and a measured field longitudinal field flatness of $\pm$1%.

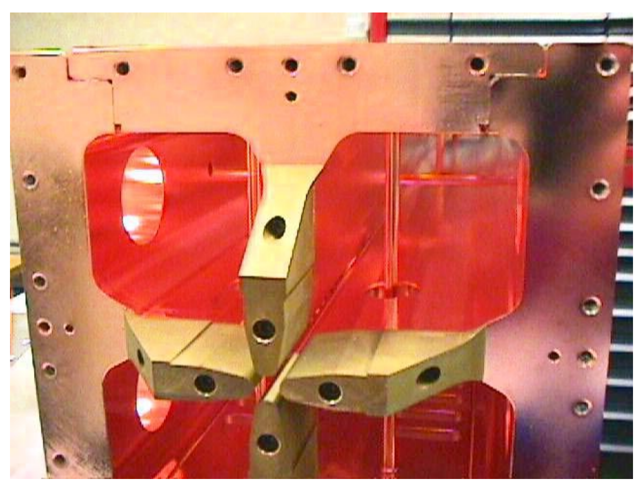

Figure 4: Cold Model End Detail, with Stabilizer

The RFQ mechanical design incorporates four separate vane quadrants which are brazed together to create the final cavity configuration. This design eliminates the need for demountable rf joints in regions of high rf wall currents. The vanes and cavity walls are made from OFE copper and they are backed by a brazed-on one inch thick piece of Glidcop AL-15©. Cooling water channels will be milled into the OFE prior to brazing on the Glidcop. Four of the 93 cm long completed modules will be joined using bolted joints with vacuum and rf seals. This method is acceptable since the longitudinal rf currents across the interfaces will be much lower than the azimuthal currents in each module. Rather than a flanged connection, the joint design will incorporate axial bolts inserted into recesses in the Glidcop layer. Benefits of this type of joint include higher strength, more reliable seal loading and a lower profile. Canted coil springs will be used in the area between adjoining vane tips to ensure good electrical contact.

Vacuum ports will consist of an array of slots small enough to attenuate any rf leakage. The ports will be incorporated identically in all four quadrants to ensure rf symmetry. Nearby tuners will be used to compensate the locally depressed cutoff frequency near the pumping ports, leveling out local variations in the vane tip voltage distribution. The RFQ vacuum level will be maintained in the 10^{-7} Torr range.

The RFQ mechanical design and prototype RFQ models are covered further in two other papers at this conference[7] [8].

5 MEBT

The MEBT transports the 2.5 MeV H^- beam from the RFQ to the DTL, and accommodates a fast traveling-wave clean-up chopper, supplied by LANL[9]. Three rebuncher cavities and 18 quadrupoles transport the beam over the 3.6 meter length. Nonlinear space charge emittance blowup is reduced to less than 20% by the large number of closely-spaced quadrupoles, which adiabatically taper the transverse betatron period length up at the entrance, focus the beam for the traveling-wave chopper, and then adiabatically refocus the beam into the DTL.

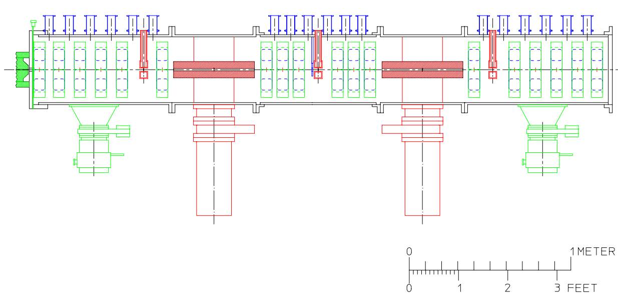

Figure 5: MEBT in Common Vacuum Chamber

The original MEBT physical configuration consisting of individual diagnostic boxes between the quadrupoles has been supplanted by a design where all components are contained inside a common vacuum chamber as shown in figure 5. Spool pieces between the beam line elements are used to maintain a low wall impedance, damping the excitation of wake fields in the vacuum chamber. The previous concept, which used a combination of EM and permanent magnet quadrupoles, has been replaced by a design incorporating only EM quadrupoles. The MEBT's high quadrupole filling factor necessitates minimizing the physical length of the magnets in order to maximize the inter-quad gaps for diagnostic devices. The associated fringe fields allow the length of an EM quadrupole to be up to one aperture radius shorter than an equivalent PM quad. To provide steering, six of the quadrupoles will be equipped with additional trim windings to create magnetic dipole fields of up to 0.03 T. All coils will be wound with solid conductor and the cores will be water-cooled.

The quadrupoles will be locally aligned to each other in groups of six on three separate strong-back structures. Mechanisms for mounting and aligning the individual strong-backs within the vacuum chamber will be provided. A distributed pumping system will be used to achieve a pressure of less than 5×10^{-8} Torr at the DTL entrance. The MEBT vacuum will be isolated from the RFQ and DTL by a pair of thin gate valves.

MEBT diagnostics will include two-slit emittance devices, Faraday cups, beam position monitors and a beam calorimeter. Additionally, toroidal beam transformers, capacitive phase probes and profile monitors will be used during routine operation of the neutron source since they are non-intercepting diagnostics.

6 ACKNOWLEDGEMENTS

The authors wish to thank Rick Gough, Craig Fong and Ron Yourd for their leadership. In addition the authors thank Jim Ayers, Don Williams, and the many other support persons who participated in this work.

7 REFERENCES

[1] John W. Staples, "The NSNS Front End Accelerator System", PAC97, May 1997, Vancouver.

[2] M.A. Leitner, R.A. Gough, K.N. Leung, M.L. Rickard, P.K. Scott, A.B. Wengrow, M.D. Williams, D.C. Wutte, Rev.Sci.Instrum. 69, 962 (1998).

[3] M.A. Leitner, D.C. Wutte, K.N. Leung, 2D Simulation and Optimization of the Volume H^- Ion Source Extraction System for the Spallation Neutron Source Accelerator, to be published in Nucl.Instrum. Methods A

[4] M.A. Leitner, D.C. Wutte, K.N. Leung, Rev.Sci.Instrum. 69, 965 (1998).

[5] M.A. Leitner, K.N. Leung, Optimization of the Volume H^- Ion Source Extraction System for the Spallation Neutron Source Accelerator Utilizing 3D Magnet and Ion Optics Codes, to be published in Nucl.Instrum. Methods A

[6] A. Ueno et al,. "Beam Test of the Pre-Injector and the 3-MeV H^- RFQ with a New Field Stabilizer PISL", Linac 96, August 1996, Geneva.

[7] A. Ratti et al,. "Conceptual Design of the SNS RFQ", Paper MO4090, Linac 98, August 1998, Chicago.

[8] A. Ratti et al,. "Prototype Models for the SNS RFQ", Paper MO4084, ibid.

[9] S. Kurennoy, J. Power, "Development of a Fast Traveling Wave Beam Chopper for the SNS Project", Paper TH4023, ibid.